General Disclaimer

One or more of the Following Statements may affect this Document

- This document has been reproduced from the best copy furnished by the organizational source. It is being released in the interest of making available as much information as possible.

- This document may contain data, which exceeds the sheet parameters. It was furnished in this condition by the organizational source and is the best copy available.

- This document may contain tone-on-tone or color graphs, charts and/or pictures, which have been reproduced in black and white.

- This document is paginated as submitted by the original source.

- Portions of this document are not fully legible due to the historical nature of some of the material. However, it is the best reproduction available from the original submission.

NASA Technical Memorandum 69366

C-Band Radar Pulse Doppler Error Its Discovery, Modeling, and Elimination

W.B. Krabill
D.J. Dempsey

February 1978

National Aeronautics and
Space Administration

Wallops Flight Center
Wallops Island, Virginia 23337
AC 804 824-3411

NASA Technical Memorandum 69366

C-Band Radar Pulse Doppler Error
Its Discovery, Modeling, and Elimination

W.B. Krabill
Wallops Flight Center
Wallops Island, Virginia

and

D.J. Dempsey
RCA
Missile and Surface Radar Division
Moorestown, New Jersey

National Aeronautics and
Space Administration

Wallops Flight Center
Wallops Island, Virginia 23337
AC 804 824-3411

TABLE OF CONTENTS

LIST OF TABLES

LIST OF ILLUSTRATIONS

C-BAND RADAR PULSE DOPPLER ERROR: ITS DISCOVERY, MODELING, AND ELIMINATION

1.0 INTRODUCTION AND BACKGROUND

The C-Band Radar Investigations performed as a part of the GEOS-3 Satellite Program undertook as one of its tasks the evaluation of the range rate tracking data obtained from those C-Band radars which have a pulse Doppler tracking capability. The GEOS-3 satellite was instrumented with a coherent C-Band transponder and this instrument was used to acquire the necessary pulse Doppler tracking data.

During the post-launch satellite check-out phase of the GEOS-3 program, data reduction and analysis efforts resulted in the discovery of a Doppler error that was a function of the target's radial acceleration from the radar (see Figure 1). Since the radar Doppler tracking servo system is of second order (i.e. two integrations), it should not have exhibited any error as a function of the first derivative ($\ddot{R}$) of the tracked parameter ($\dot{R}$). Thus the observed $\ddot{R}$ dependent tracking error was both unexpected and initially unexplainable.

Following a series of special experiments, it was further discovered that the observed error was also inversely proportional to the radar's operating Pulse Repetition Frequency (PRF) (see Figure 2). That is, the error was approximately four times larger at a PRF of 160 per second than it was at a PRF of 640 per second. This PRF dependency led to an investigation into, and analysis of, the effects of using a finite sampling rate to update the tracking loop's local oscillator. The tracking loop in question (see Figure 3) is a sampled data system in which the radar's local oscillator consists of a digitally controlled frequency synthesizer which is updated once each PRF to bring its frequency into agreement with the observed target's Doppler return as measured by a continuously tracking Doppler frequency counter.

The results of the initial analysis indicated that the local oscillator's finite update rate was indeed the source of the error and that its magnitude would, for a constantly accelerating target follow the relationship:

$$\varepsilon(\dot{R}) = \frac{\ddot{R}}{2\ PRF} = \frac{PRI}{2}\ddot{R} = \frac{T}{2}\ddot{R}$$

where T = frequency synthesizer sampling interval.

Thus, the error follows the general relationship:

$$\Delta\dot{R} = \ddot{R}\,\Delta t$$

from which it can be seen that the $\frac{PRI}{2}$ factor actually acts as an apparent time shift.

The validity of the error model was tested by time shifting the radar's Doppler measurements by an amount:

$$t' = t + \Delta t = t + \frac{PRI}{2}$$

That is, the corrected time tag for the Doppler data was made equal to the recorded time tag plus a Δt factor of $\frac{PRI}{2}$ while all other radar measurements (range and angles) retained their original time tags.

After implementing the above described data time shift corrections, orbital analysis using GEOS-3 C-Band tracking data showed that the previously noted tracking error was no longer present (see Figures 10 and 11).

Subsequent rigorous math modeling of the tracking loop verified the completeness of the original error model and the development of a hardware "fix" provides a method for reducing the error, in real time, to a negligible, small value.

Since all have similar implementations, all RCA designed C-Band pulse Doppler systems (installed/designed into AN/FPQ-6, AN/TPQ-18, AN/FPS-16 and AN/MPS-36 Radars) will exhibit an identical $\frac{T}{2}$ dependent Doppler error. Likewise, the error correction techniques described in Section 3 are applicable to all these C-Band pulse Doppler systems.

1.1 OBSERVED RANGE RATE RESIDUAL ERROR

The GEOS-3 C-Band radar investigations utilize orbital analysis techniques to quantitatively evaluate the performance of the world-wide network of C-Band instrumentation radars. The computer program used for orbit generation purposes is referred to as GEODYN. This orbit generation program was developed by Wolf Research and Development Corporation and has been in use at the NASA Wallops Flight Center throughout both the GEOS-2 and GEOS-3 Satellite Programs.

NASA-WFC has had almost 10 years of experience with this orbital generation and analysis technique and its ability to generate highly accurate orbits has been amply demonstrated.

For radar data analysis and evaluation purposes, the radar data are processed by GEODYN and a reference orbit for the satellite is generated. This orbit is, for radar data analysis purposes, assumed to be perfect. Thus, this orbit is used as the reference for determining what the radar R, A, E, and $\dot{R}$ measurements should be as a function of time. Any deviation of the actual radar measurements from the orbitally derived "True" set are then considered to be residual radar measurement errors.

Figure 1 is a plot of range rate residual errors as observed in the tracking data from the Wallops Island AN/FPQ-6 Radar for revolution number 212 of the GEOS-3 Satellite. In this figure, the zero error line represents an ideal track condition where both the range rate as derived from the orbital solution and the actual radar measurements agree exactly. Any deviation of the measured data from this ideal, zero-error state is then plotted as a radar range rate residual error. It can be seen in Figure 1 that this residual error on Rev. 212 starts and ends near zero and peaks up to a value of approximately +17 cm/sec near the center (point of closest approach - PCA) of the track. This resulting bell shaped curve is of the same form as the range acceleration curve for a radar tracking an orbiting body. This set of residuals led to the initial conclusion that the C-Band Doppler data was exhibiting an apparent range accleration dependent error.

It is common practice in the design and analysis of servo control systems to define a set of steady state dynamic lag error coefficients as:

$$\varepsilon(\theta) = \frac{\dot{\theta}}{K_v} + \frac{\ddot{\theta}}{K_a} + \frac{\dddot{\theta}}{K_j} + \ldots$$

For a range rate loop this can be written as:

$$\varepsilon(\dot{R}) = \frac{\ddot{R}}{K_v} + \frac{\dddot{R}}{K_a} + \ldots$$

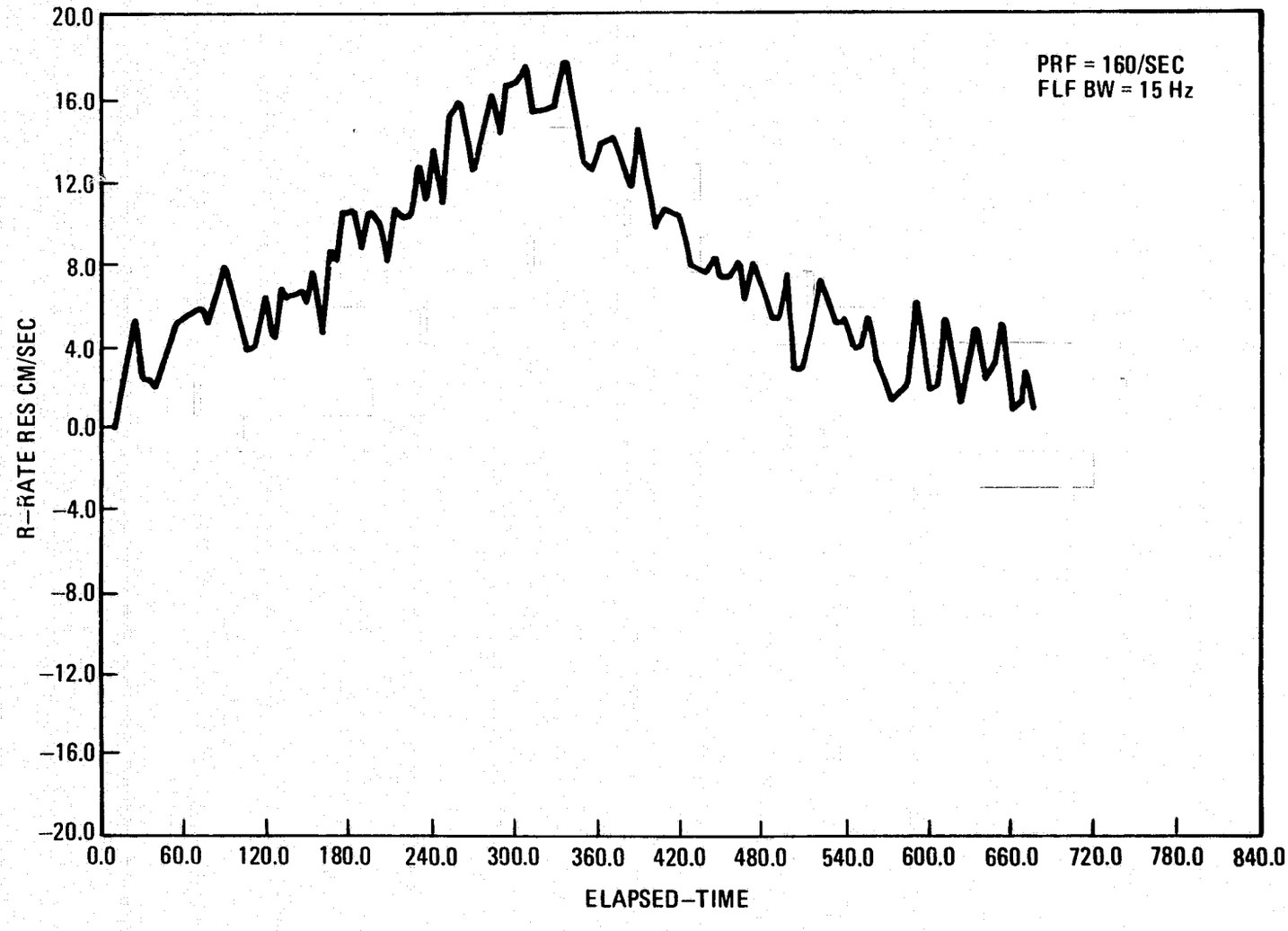

Figure 1. - Range rate residual error GEOS-3, Rev 212

where it is noted that the range acceleration dependent term is associated with the velocity constant K_v. In a properly functioning type 2 loop, this velocity constant has a magnitude which is essentially infinite. Therefore, no range acceleration dependent lag error should exist in a type 2 range rate servo loop.

There was the possibility, of course, that the error was arising due to a malfunctioning of the loop. However, at-site tests indicated that the loop was performing in a satisfactory fashion.

1.2 OBSERVED ERROR DEPENDENCE UPON RADAR PRF

The resulting dilemma remained unresolved for a few weeks until orbital analysis was completed on another set of tracking data from revolution number 498 (see Figure 2). This particular pass of the satellite (498) was used to conduct some special radar tests during which the normal radar operating PRF of 160 per second was used in the beginning and end of the track and a higher PRF of 640 per second was used for about one minute during the center portion of the track.

Orbital analysis of the range rate data from revolution 498 is shown in Figure 2. A review of these data led to the rather obvious conclusion that the range rate error is PRF dependent. This dependency is evidenced by the sharp drop in the magnitude (4:1 reduction) of the residual error near elapsed time 330 when the PRF was changed from 160 to 640. The return to a PRF of 160 again one minute later is associated with a corresponding return to a higher range rate error. In the end, it was this PRF dependence which proved to be the key to resolving the source of the previously noted range rate error.

2.0 ERROR MODELING

The observed GEOS-3 C-Band radar Doppler tracking error is discussed, modeled and interpreted in this section.

The modeling and discussion is presented in two parts. First, a mathematically rigorous model of both the tracking loop and resulting tracking error is presented in Section 2.1. This mathematical analysis is presented

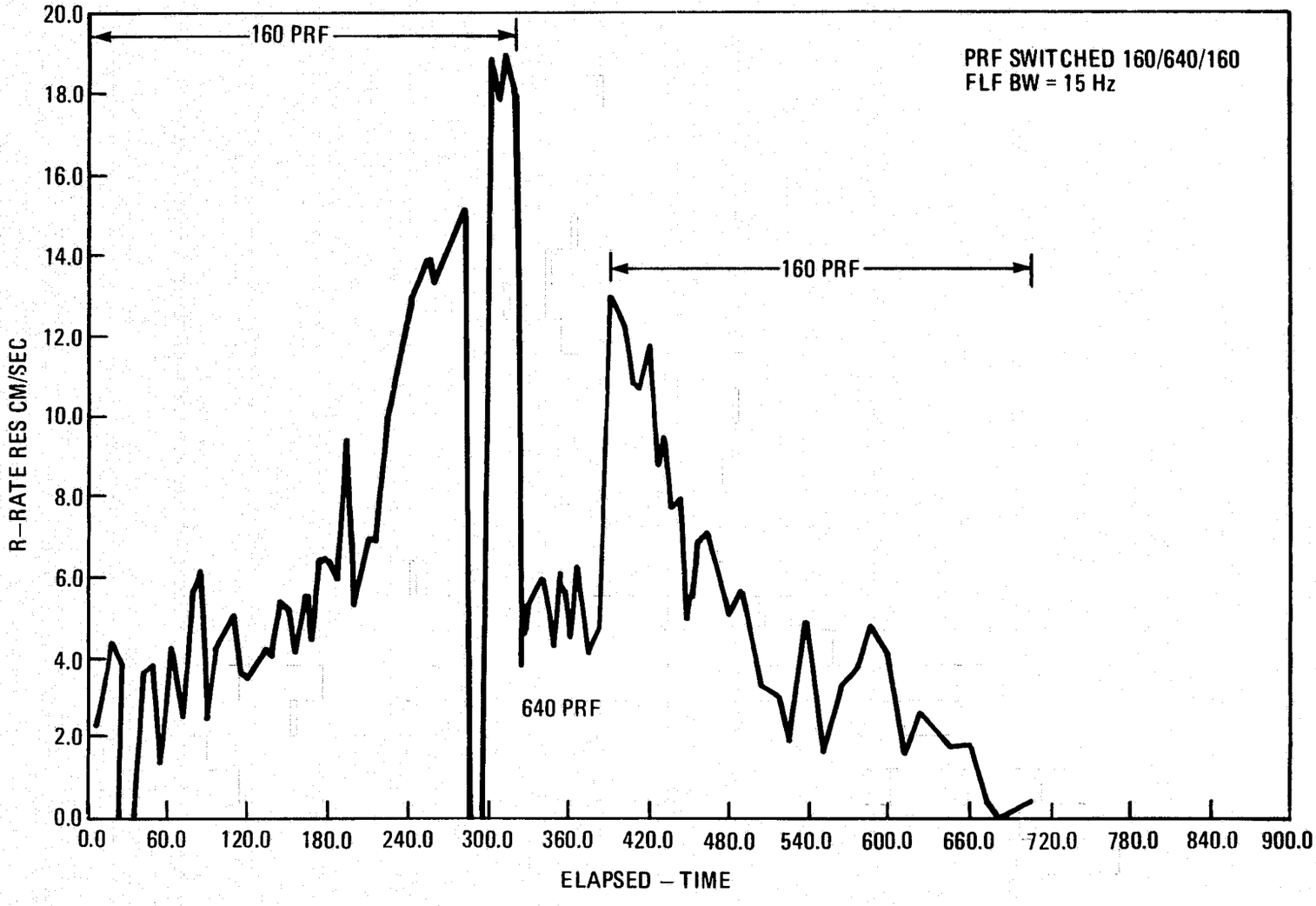

Figure 2. - Range rate residual error GEOS-3, Rev 498

for both the case of a target having a constant radial range acceleration ($\ddot{R}$) and then for a target having a constant range jerk ($\dddot{R}$). The results of the analysis for these two cases are then interpreted and, for the general case, it is shown that if the loop data are sampled at a time $\frac{T}{2}$ seconds prior to its utilization (time tag), the resulting Doppler measurement is accurate to within a small constant error. This is, of course, the equivalent of sampling the data at the desired time and then modifying the data word time tag by an amount:

$$\text{Data Time Tag} = \text{Sample Time Word} + \frac{T}{2} \text{ seconds}$$

The mathematical analysis of the Doppler error as developed in Section 2.1 is augmented by a graphical analysis and discussion in Section 2.2. This latter approach will provide the less mathematically-inclined reader with a further insight into the form and source of the observed error. This latter approach will also be useful in developing practical error correction techniques. The reader may find it useful to review Section 2.1 after having read the discussion of Section 2.2.

2.1 MATHEMATICAL MODELING AND ANALYSIS

Linear servo theory tells us that a type 2 feedback loop* can follow a ramp input precisely, exhibiting no steady-state error. So, too, do we expect a type 2 Doppler tracker to perfectly follow the linearly increasing Doppler frequency that arises from a range accelerating target. The C-Band radar Doppler tracker[1] is effectively linear. It is a discrete time system, however, in that the feedback frequency is generated by a frequency synthesizer as opposed to a continuous-response voltage controlled oscillator. When this tracker is locked onto the satellite, an error due to target acceleration (that is, having the same profile as the acceleration) has consistently been observed, hence apparently contradicting the result predicted from servo theory.

The identification of the root of this paradox and the development of the mathematical model to properly account for the observed results is the subject of this section. It is written in the context of GEOS-3 doppler track data; however, the analysis is perfectly applicable to any phase or frequency loop in which the feedback signal is generated from a frequency synthesizer.

* - A type 2 feedback loop is one characterized by a double integration in the forward path.

2.1.1 MATHEMATICAL MODEL

A simplified block diagram of the radar Doppler tracking loop is shown in Figure 3. This is derived from the description given in Reference 1. It is desired to determine the steady-state response of the tracker due to stimuli of linearly and quadractically increasing Doppler frequencies.

In reducing the block diagram to a mathematical model, it would be incorrect to assume that the frequency discriminator can be characterized as a simple gain factor, converting frequency into a d.c. voltage. Rather, the more generalized concept of frequency as the derivative of phase angle must be invoked. The problem is precisely this. Consider a C.W. waveform that is constant in frequency but that undergoes a step discontinuity of Δ in phase every T seconds. That is

$$f(t) = \cos 2\pi ft + n\Delta , \quad nT < t \leq (n+1)\, T \tag{1}$$

for n = 0, 1, 2, ---. The circuitry downstream from this signal will follow it by smoothing out the discontinuity and "catching up" until the response is right for the current phase angle of the input. Assuming that the transient dies out within T, the average frequency in radians per second of the response signal during each interval is

$$\frac{\Delta \emptyset}{\Delta t} = \frac{2\pi fT+\Delta}{T} = 2\pi f + \Delta/T \tag{2}$$

That is, paradoxically, even though the stimulus has constant instantaneous radian frequency $2\pi f + \Delta/T$. Any integration process would clearly respond to this average value. It is not necessary to know the exact shape of the smooth-out transient in a sampled data system such as the Doppler tracker because the values processed at the sampling instants are analogous to the average values that occur during the corresponding integration interval of the associated continuous system.

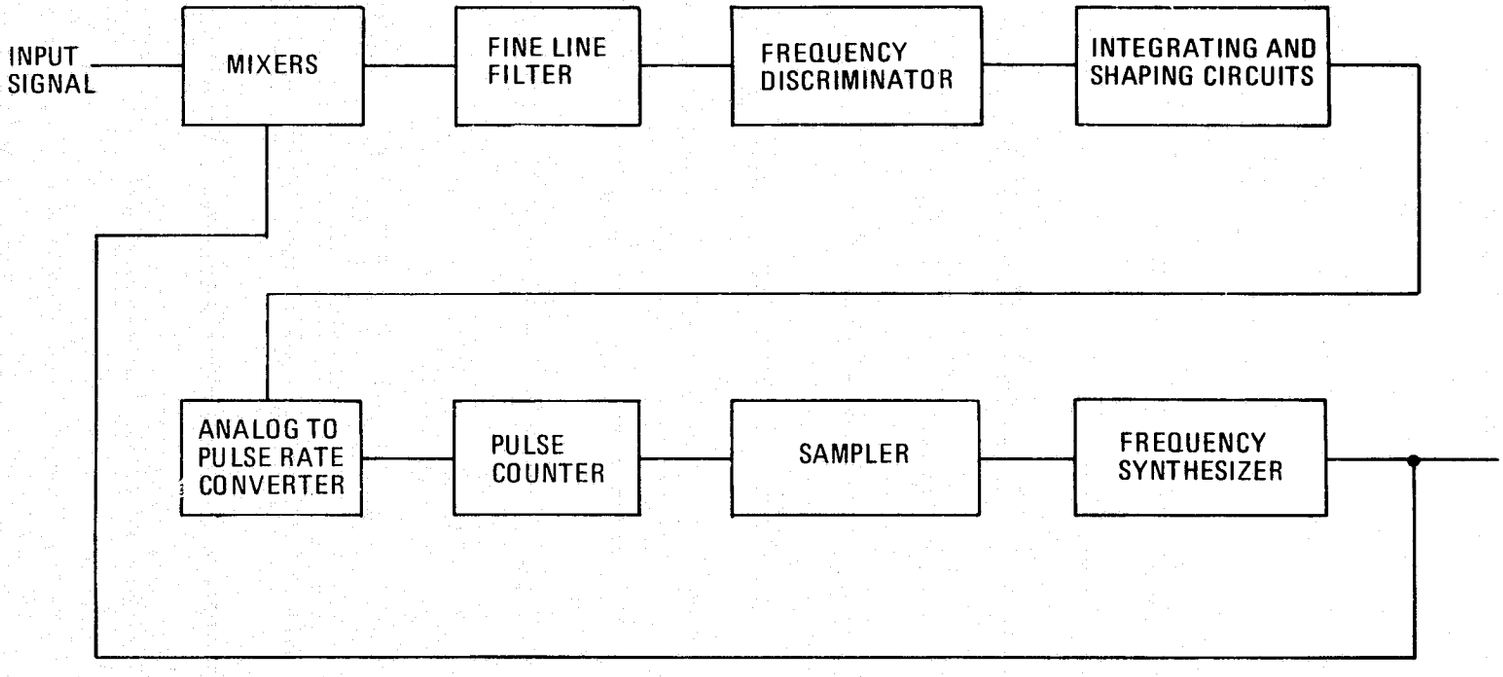

Figure 3. - Simplified block diagram of the C-Band radar Doppler tracking loop

In order to properly account for the phenomenon described, it is necessary to model the frequency discriminator as a device that differentiates phase angle and then converts the resulting parameter to a d.c. signal. But this further requires that instead of processing frequency, one has to model the loop in terms of phase. Referring to Figure 3, the error frequency out of the mixers is effectively sampled and held by the fine line filter. During this interval the phase angle, being the integral of frequency, is increasing linearly. This process is described at the loop input by simultaneously sampling frequency and phase; then during the pulse repetition interval, integrating the former (converting to phase), holding the latter, and combining the result. The feedback frequency is effectively sampled and held (zero order) by the synthesizer. Phase, then is merely the integral of this frequency. The phase error is formed and input to the discriminator where, as indicated, it is differentiated and converted to an analog voltage representing frequency. Thereafter the signal is integrated twice (a type 2 loop) before it is sampled and fed back by the frequency synthesizer. Since only the steady-state performance is of interest, the shaping circuits that are required for stability will be ignored. They contribute nothing in the steady-state. Also, the synthesizer actually "samples" the frequency a small interval δ prior to the arrival of the next radar pulse. This, however, is not a factor in this analysis and will also be ignored. The S-plane model thus derived is shown in Figure 4. The transfer function of the zero order hold is

$$H(S) = \frac{1}{S}\left(1-e^{-TS}\right) \tag{3}$$

In this form it is possible to convert to Z transforms and express the loop response directly. The result is

$$C(Z) = \frac{G_1G_3(Z)R_1(Z) + G_2G_3(Z)R_2(Z)}{1 + HG_3(Z)} \tag{4}$$

The frequency input is denoted by $R_1(Z)$ and the phase input by $R_2(Z)$.

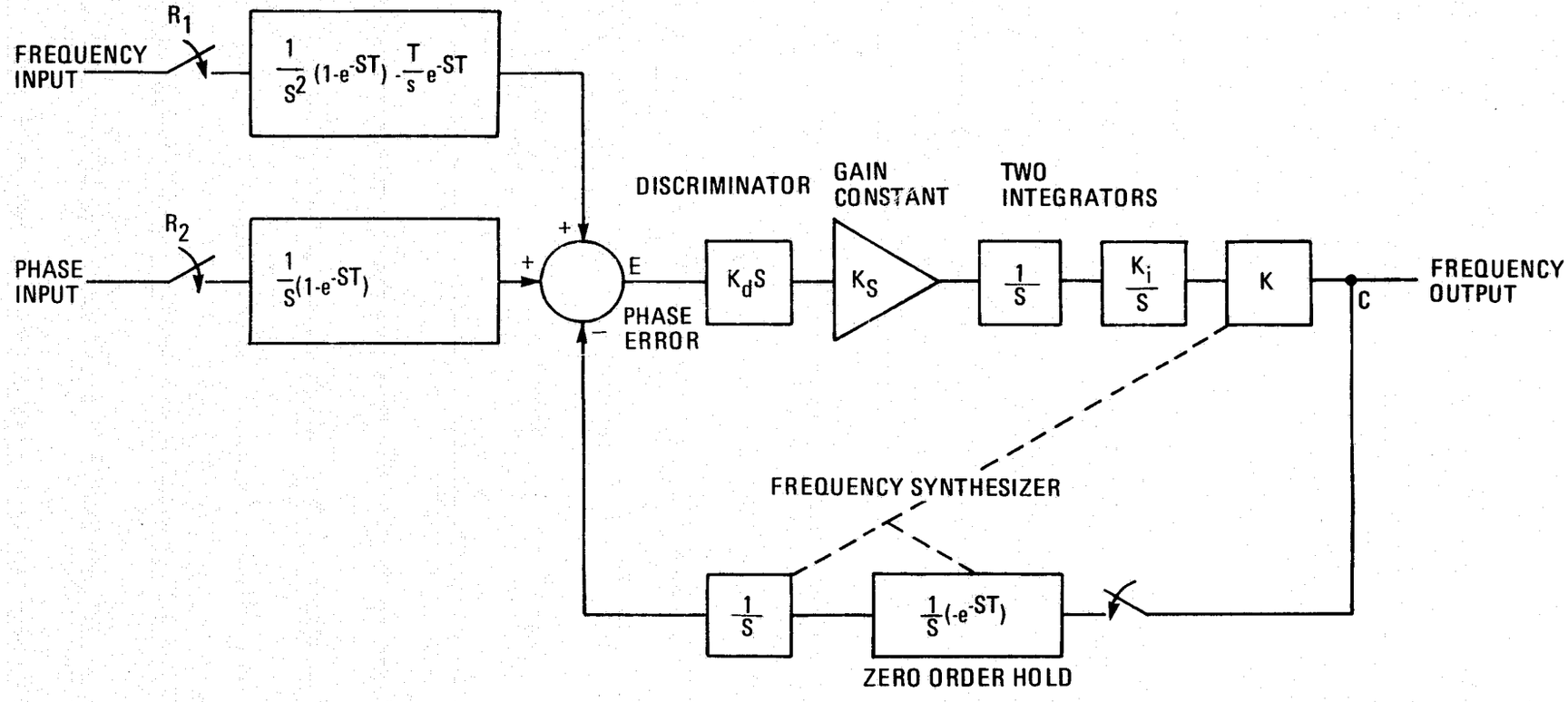

Figure 4. - S-Domain model of the Doppler tracking loop

Additionally, $G_1G_3(Z)$ denotes the Z transform of the tandem combination of

$$\left[\frac{1}{S^2}(1-e^{-ST}) - \frac{T}{S}e^{-ST}\right] \cdot \frac{K_a}{S},$$

$G_2G_3(Z)$ means the Z transform of

$$\left[\frac{1}{S}(1-e^{-ST})\right] \cdot \frac{K_a}{S},$$

and $HG_3(Z)$ denotes the Z transform of

$$\left[\frac{1}{S^2}(1-e^{-ST})\right] \cdot \frac{K_a}{S} \tag{5}$$

In each of these expressions, K_a is set to the product $K_dK_sK_iK$. These expressions are all found with the aid of the table of Z transforms, p. 60 of Reference 2 and the transform,

$$1-e^{-TS} \rightarrow 1-Z^{-1} = \frac{Z-1}{Z} \tag{6}$$

The results are

$$G_1G_3(Z) = \frac{K_a[T^2(Z+1)-2T^2]}{2(Z-1)^2} \tag{7}$$

$$G_2G_3(Z) = \frac{K_aT}{Z-1}, \tag{8}$$

and

$$HG_3(Z) = \frac{T^2(Z+1)K_a}{2(Z-1)^2} \tag{9}$$

2.1.2 LINEAR FREQUENCY INPUT

We are primarily interested in the steady state frequency error, that is, the loop output denoted by C in Figure 4 minus the input frequency. Equation (4) gives C(Z) as a function of the inputs $R_1(Z)$ and $R_2(Z)$. Consider first the case of an input frequency that is linearly increasing with time,

$$f = qt \tag{10}$$

where q is in hertz per second. Input phase in cycles, being the integral of (10), is

$$\phi(t) = 1/2\ qt^2 \tag{11}$$

Again resorting to p. 60 of Reference 2 for the Z transforms,

$$qt \rightarrow \frac{qTZ}{(Z-1)^2}\ , \text{ and}$$

$$1/2\ qt^2 \rightarrow \frac{qT^2Z\ (Z+1)}{2(Z-1)^3} \tag{12}$$

Using (4), (7) through (9) and (12), the Z transform of the frequency error is

$$F(Z) = \frac{K_a\ \frac{T^2(Z+1)-2T^2}{2(Z-1)^2}\quad \frac{qTZ}{(Z-1)^2} + \frac{K_aT}{Z-1}\quad \frac{qT^2Z(Z+1)}{2(Z-1)^3}}{1 + \frac{K_aT^2(Z+1)}{2(Z-1)^2}} - \frac{qTZ}{(Z-1)^2} \tag{13}$$

And finally, the steady state value is available from the final value theorem, p. 71 of Reference 2:

$$\lim_{t \rightarrow \infty} f(t) = \lim_{Z \rightarrow 1} \frac{Z-1}{Z}\ F(Z) \tag{14}$$

After simplification, (14) reduces to

$$\lim_{t\to\infty} f(t) = \lim_{Z\to 1} \frac{qK_aT^3 - 2qT(Z-1)}{2(Z-1)^2 + K_aT^2(Z+1)} \qquad (15)$$

$$= \frac{qT}{2}$$

Equation (15) indicates that under the influence of an input frequency ramp (target having constant acceleration), the loop leads the input frequency by a constant amount qT/2 Hz. Since the input frequency is increasing by q Hz/sec, it follows that the loop response anticipates the input frequency by T/2 seconds.

The Doppler frequency returned by a target having constant radial velocity v is

$$f = \frac{2v}{c} f_t \qquad *(16)$$

where c is the speed of light and f_t is the transmitted frequency. Differentiating both sides of (16) and letting $\dot{f} = q$,

$$q = \dot{f} = \frac{2\dot{v}}{c} f_t \qquad (17)$$

where the $(\dot{})$ denotes first derivative. We may determine the error in radial velocity corresponding to an error of

$$f = \frac{qT}{2} \text{ Hz.} \qquad (18)$$

Solving (16) for v and using (17) and (18), there obtains

$$v = \dot{v}\, T/2 \qquad (19)$$

For an 87° elevation pass, $\dot{v}$ at the point of closest approach is approximately 50 meters/sec^2. Assuming a PRF of 160/sec,

$$v = 15.6 \text{ cm/sec} \qquad (20)$$

error in the measured target radial velocity.

*Equation 16 is an approximation. Its use in the sequel will introduce negligible error.

One word of caution is required. The mathematical model used here assumes that the phase discontinuity cited in (1) and (2) and the continuation is always positive; i.e.,that the average frequency is always thereby increased. This is surely the case for small phase steps. However, as this discontinuity becomes greater than 180°, it is reasonable to expect that instead of "catching up", downstream circuitry will retard, slowing down to accommodate the current phase angle. Average frequency will, in that case, be less than the instantaneous value. As the phase step approaches 360°, it is easy to see that no transient at all will be induced. Therefore it is necessary to confirm that for the radar tracking loop this phase step is significantly smaller than 180°. Again assume the input frequency is expressed as qt. The phase step seen by the discriminator will be the difference in the phase excursion each pulse repetition interval (PRI) between the input and feedback signals. The phase excursion of the input is

$$\phi_i = \int_{nT}^{(n+1)T} qt\, dt$$

$$= 1/2\, qt^2 \Big|_{nT}^{(n+1)T} = q\,T^2\, n + 1/2\, q\,T^2 \qquad (21)$$

Assume the case in which the feedback is following the input perfectly. Then at time nT the frequency out of the synthesizer is held at qnT and the phase change during the next PRI is

$$\Delta\phi_f = (q\ nT)\ T = qnT^2 \qquad (22)$$

Therefore, the phase discontinuity at the next sample instant is

$$\Delta\phi = \Delta\phi_i - \Delta\phi_f = 1/2\ q\ T^2 \qquad (23)$$

Using (17), a typical maximum acceleration of 50 m/sec^2, a C-band transmission frequency of 6 Gigahertz, and a PRI of 160/sec,

$$\Delta\phi = 14°$$

which is seen to satisfy the requirement and validate the model.

2.1.3 QUADRATIC FREQUENCY INPUT

Consider now the case in which the target motion is characterized by constant jerk. Its Doppler frequency will then appear as a quadratic,

$$f = bt^2 \tag{24}$$

and the associated phase, a cubic

$$\phi = 1/3\ bt^3 \tag{25}$$

The corresponding Z transforms of (24) and (25) are

$$bt^2 \rightarrow \frac{bT^2\ Z\ (Z+1)}{(Z-1)^3}\ , \text{ and}$$

$$1/3bt^3 \rightarrow \frac{bT^3\ Z\ (Z^2 + 4Z+1)}{3\ (Z-1)^4} \tag{26}$$

(notice that entry 1.04 in the Table of Z Transforms, p. 588 of Reference 3 is incorrect.) Using (26) in (4) to determine the steady-state loop error as was done for the constant acceleration (linear Doppler) case leads to the conclusion that the frequency error becomes infinitely large under constant jerk. It is, however, possible to determine the rate at which the error increases. What is needed is the steady-state value of the first difference. But the first difference of any function expressed as a Z transform, F(Z), is readily available as

$$(Z-1) \cdot F(Z) \tag{27}$$

Then, using (26), (27), and (4) in (14), the final value of the first difference of the frequency error under constant target jerk is

$$\lim_{Z\to 1} \frac{Z-1}{Z}(Z-1)\frac{\frac{K_aT^2(Z-1)}{2(Z-1)^2}\frac{bT^2Z(Z+1)}{(Z-1)^3}+\frac{K_aT}{Z-1}\frac{bT^3Z(Z^2+4Z+1)}{3(Z-1)^4}}{1+\frac{K_aT^2(Z+1)}{2(Z-1)^2}}-\frac{bT^2Z(Z+1)}{(Z-1)^3}$$

$$= \lim_{Z\to 1} \frac{1/3\ K_abT^4\ 2(Z+2) - 6\ bT^2(Z+1)(Z-1)}{2(Z-1)^2 + K_aT^2(Z+1)} \qquad (28)$$

$$= bT^2$$

Hence, the Doppler tracking loop will lead the input frequency under constant jerk by an amount increasing at the rate of bT^2 Hertz per pulse repetition interval (PRI). It was postulated that the true target Doppler frequency equals bt^2. Equation (28) indicates that the frequency of the tracker, denoted by C in Figure 4, increases as $bt^2 + bTt$ (hence a difference of bTt or bT^2 each PRI). At what time difference, X, shall we monitor the tracker to get the best estimate of the input frequency?

$$b(t-x)^2 + bT\ (t-x) = bt^2$$

$$bt^2 + bt\ (T-2x) \quad b\ (x^2-Tx) = bt^2 \qquad (29)$$

Letting x=T/2 (that is, monitoring the loop frequency T/2 seconds prior to the arrival time of the radar return) gives the input frequency to within a constant error. In all likelihood this error will be dominated by the acceleration steady-state error of the analogous continuous type 2 servo. The time shift, T/2, is consistent with the value derived under the influence of a constant accelerating target.

The error derived here may be re-interpreted in terms of target velocity. Starting from (16), we have

$$\dot{f} = \frac{2\dot{v}}{c} f_t, \text{ hence}$$

$$\Delta f = \frac{2\Delta v}{c} f_t, \text{ and} \qquad (30)$$

$$\ddot{f} = \frac{2\ddot{v}}{c} f_t. \qquad (31)$$

Differentiating (24) twice and substituting in (31), and setting (30) equal to bT^2 per PRI leads to

$$\Delta v = \frac{\ddot{v}T^2}{2} \quad . \tag{32}$$

For an 87° pass, maximum $\ddot{v}$ is approximately 0.3 meters/sec^3. For a PRI of 160, (32) gives the velocity error as equal to 0.0006 cm/sec per PRI. These results, of course, apply only so long as the acceleration induced by the jerk causes a phase discontinuity that is small compared with 180° as discussed previously.

2.2 GRAPHICAL ANALYSIS AND DISCUSSION OF THE $\frac{PRI}{2}$ ERROR

2.2.1 Target with Constant Range Acceleration

To gain a further insight into the operation of the radar's Doppler loop and the source of the observed $\frac{PRI}{2}$ error, consider again the case of a target which exhibits a constant radial range acceleration component. This target would produce a Doppler frequency which is a linearly increasing function of time. For convenience, assume that the magnitude of the range acceleration is such that the Doppler frequency exhibits a slope which is 0.1 Hz/second. Also for convenience, assume a radar PRF of only 10 per second so that the Pulse Repetition Interval (PRI) is 0.1 seconds. Finally, assume that the target has been previously acquired and that a stable Doppler track condition exists.

Based upon the previous discussion of the Doppler loop (Figure 3) operation, it is expected that the Doppler frequency counter is perfectly tracking the hypothetical target's Doppler frequency. Thus, it is assumed that the contents of this counter agree exactly to the ideal Doppler frequency associated with the target's range rate at any given instant of time. In line with previous discussions, the contents of the Doppler counter are extracted once each PRF (i.e. 10 times per second for this simplified case) and used to set the local oscillator (LO) frequency synthesizer to the expected target return Doppler frequency. If as assumed a perfect Doppler track is occurring, the LO to target return frequency comparison will result in a zero frequency error indication at the output of the loop's frequency discriminator and the loop, using its stored velocity estimate, will continue to track in an ideal fashion.

Figure 5 depicts the operation of the Doppler tracker for the assumed target conditions. In this figure, the solid line represents the true target Doppler. Due to the assumed perfect track (zero frequency error) conditions, this same solid line must also represent the contents of the Doppler counter. The dashed line represents the assumed periodic (10 times per second) updating of the local oscillator (frequency synthesizer).

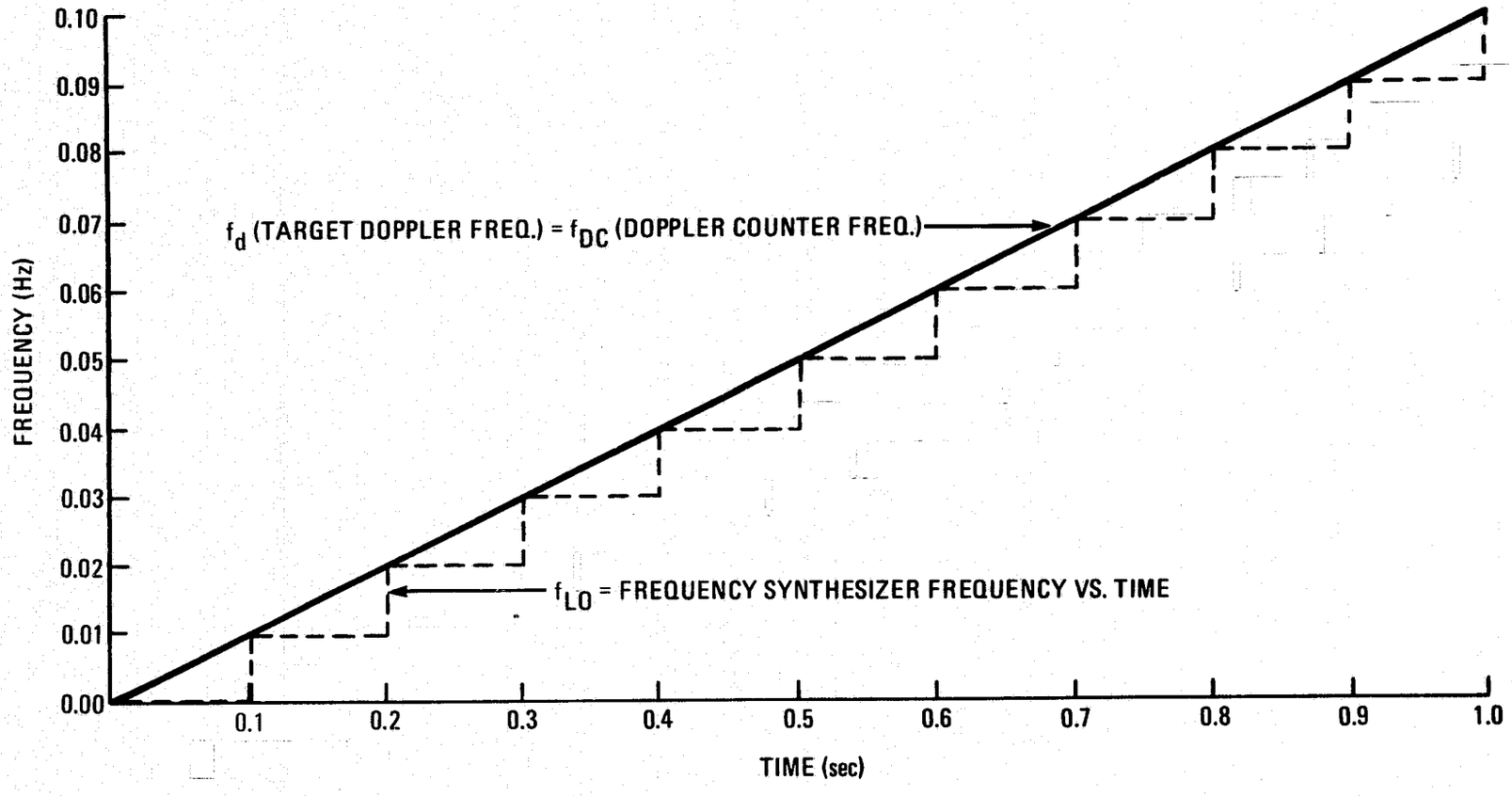

Figure 5. - Loop frequency relationships for original model

This model of loop operation appears to satisfy the conditions for stable loop operation. The synthesizer will ideally provide an LO frequency which will match the target's Doppler frequency exactly and all seems well. However, knowing that the loop actually exhibits an error leads to a more in-depth look into its operation.

To understand the source of the observed error, it is necessary to recall that frequency and phase are related by

$$\omega = \frac{d\phi}{dt}$$

Thus the assumed zero frequency error will only occur if the local oscillator's phase versus time profile is either matched to, or constantly offset from, the phase versus time profile of the target's Doppler frequency. That is,

$$(\omega_{LO} - \omega_d) = (\dot{\phi}(t)_{LO} - \dot{\phi}(t)_d) = 0$$

if and only if

$$(\phi(t)_{LO} - \phi(t)_d) = \text{zero or a constant}$$

The solid curve of Figure 6 depicts the phase profile generated by the assumed constantly accelerating target. The form of the phase profile is a quadratic since a linear Doppler frequency is assumed.

The dashed curve of Figure 6 is actually the composite of a series of straight lines and it represents the phase profile of the frequency synthesizer's output for the operating model presented and discussed above.

To understand the generation of the LO phase curve, recall that the synthesizer is periodically set for a desired output frequency (based upon the Doppler counter contents) and allowed to remain at this same frequency until the next update time. Thus the synthesizer output has a constant frequency between updates which, in turn, results in a linear phase profile during this inter-sampling period. At the end of the period, the synthesizer's frequency

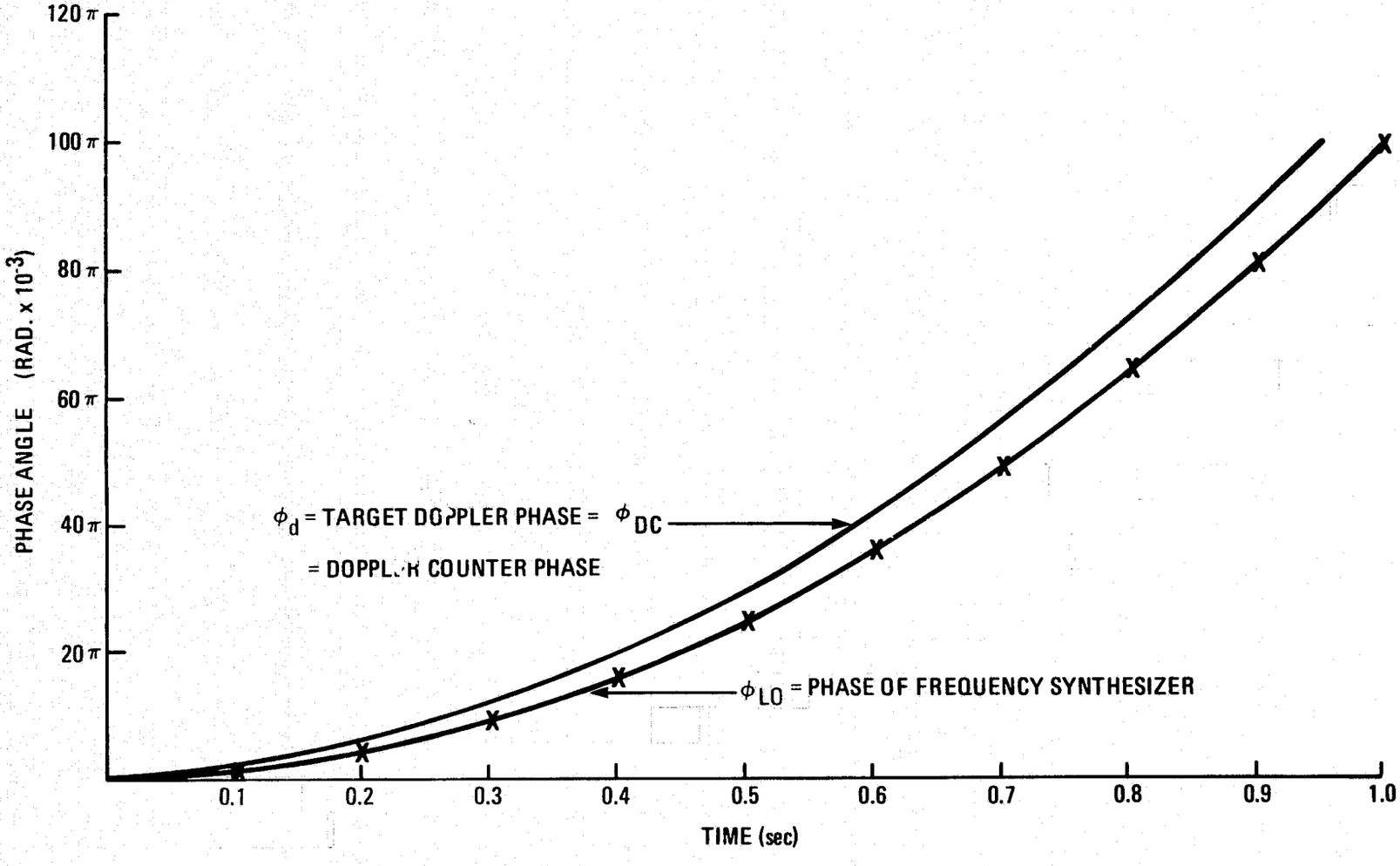

Figure 6. - Loop phase relationships for original model

is changed but the new frequency starts with an initial phase angle which is the same as the final phase angle of the previous output frequency. (A small allowable phase jitter is allowed but this is negligibly small and not of concern for the present discussion.) Thus, as shown, the synthesizer's output phase profile consists of an interconnected series of straight line segments each of which has a slope which is related to the synthesizer's fixed output frequency for that particular sampling interval.

Table 1 presents a tabulation of the phase angles of the frequency synthesizer (LO) output (ϕ_{LO}) and Doppler frequency (ϕ_d) as determined at the start of each synthesizer update interval. The instantaneous phase difference between these two phase parameters ($\Delta\phi = \phi_{LO} - \phi_d$) is also listed. It is this latter parameter ($\Delta\phi$) which is of primary significance to the present discussion. $\Delta\phi$ is plotted as a function of time in Figure 7.

Obviously, $\Delta\phi$ is a linearly decreasing (or increasing depending upon the sign convention assumed for the frequency discriminator) function of time. Such a linear phase error is the equivalent of a constant frequency error at the input to the loop. This does not meet the criteria for a zero frequency error which was the assumed steady state loop operating condition. In actual closed loop operation, the loop would react to compensate for such an error with the result that the Doppler counter will track along a curve other than originally assumed (true f_d curve). It is therefore apparent that the simple frequency-only model for loop operation is inadequate and must be modified to account for phase effects introduced by the synthesizer sampling technique.

TABLE I. Cumulative Phase and Phase Difference for Original Model

Start of PRI #	t(sec)	ϕ_{LO} (rad x 10^{-3})	$\phi_d = \phi_{DC}$ (rad x 10^{-3})	$\Delta\phi = \phi_{LO} - \phi_d$ (rad x 10^{-3})
0	0	---	---	---
1	0.1	---	π	$-\pi$
2	0.2	2π	4π	-2π
3	0.3	6π	9π	-3π
4	0.4	12π	16π	-4π
5	0.5	20π	25π	-5π
6	0.6	30π	36π	-6π
7	0.7	42π	49π	-7π
8	0.8	56π	64π	-8π
9	0.9	72π	81π	-9π
10	1.0	90π	100π	-10π

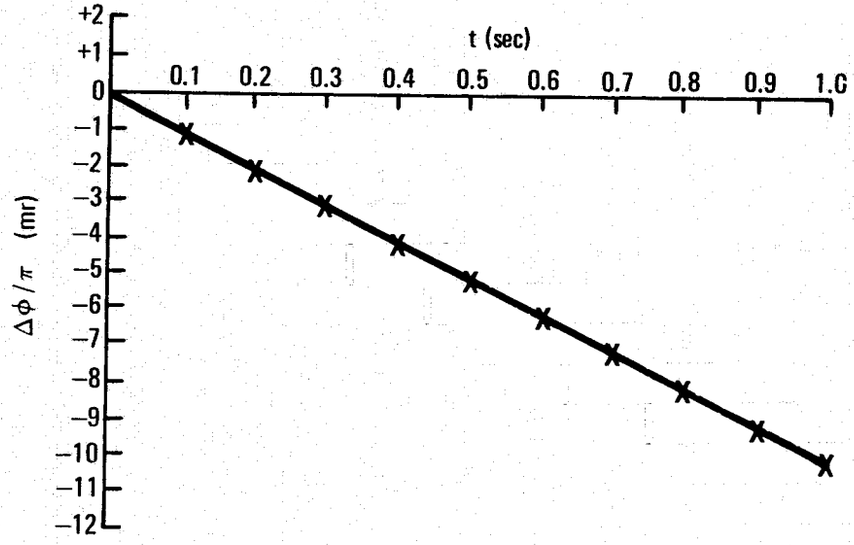

Figure 7. - $\Delta\phi$ Vs. Time (Original model)

In order to establish a modified functional model which will result in the desired zero error steady state condition, consider the input frequency error which would result from the data tabulated in Table 1. The equation of the cumulative phase difference is:

$$\Delta\phi(t) = (-\pi \times 10^{-2})t$$

Therefore, the resulting Doppler counter error would be

$$\Delta_f = \frac{1}{2\pi} \Delta\omega = \frac{1}{2\pi} \frac{\Delta\phi}{\Delta t} = \frac{-\pi \times 10^{-2}}{2\pi}$$

or

$$\Delta_f = \text{constant} = -0.5 \times 10^{-2} \text{ Hz}$$

This equation states that the loop must adjust itself to compensate for an otherwise constant input frequency error of 0.005 Hz. Referring back to Figure 5, it becomes apparent that the loop error represents the frequency difference between the Doppler curve and the <u>average</u> synthesizer output frequency. That is, the error, if superimposed on this diagram, would be a straight line passing through the frequency mid-points of the dashed synthesizer "staircase" curve.

The fact that the curve appears to be associated with the average difference frequency between the Doppler and synthesizer output leads to the conclusion that the original model would still be applicable if it is assumed that the return Doppler frequency is perfectly tracked by the average frequency out of the frequency synthesizer rather than by the Doppler counter as previously assumed. Figure 8 shows the tracking relationship which must exist if this adjustment is made to the functional model.

Referring to Figure 8, it is apparent that the zero average error condition for the frequency synthesizer has been achieved at the expense of introducing a constant measurement error into the Doppler counter. Since this Doppler counter error doesn't introduce a loop error (in fact is necessary to compensate for the previously described error), it will not affect the operation of the loop. Unfortunately, it does affect the output Doppler (range rate) measurements of the system.

Further study of Figure 8 shows that the instantaneous contents of the Doppler counter lead (in time) the true target return Doppler frequency by an amount:

$$\Delta t = \frac{\text{Sampling Interval}}{2} = \frac{PRI}{2}$$

Thus,

$$f_{DC}(t=t) = f_{TD}\ (t=t + \frac{PRI}{2})$$

where

f_{DC} = frequency of the Doppler counter

f_{TD} = true return Doppler frequency

Before ending this discussion, it is necessary to show that the modified functional model results in a synthesizer phase profile which either matches the true Doppler phase profile or is separated from it by a constant amount.

Figure 9 has been generated in the same fashion as was followed for generation of Figure 6 except that the frequency of the Doppler counter has been shifted as is required by the modified loop functional model. Table 2 provides a tabulation of the phase and frequency relationships which exist within the loop. It should be noted that the frequency synthesizer's phase is still changing in a linear fashion between update times. The scale of the figure prevents this linear change to be depicted. This linear change of the synthesizer is, however, no longer important since the resulting phase of the synthesizer at the update time is now exactly correct to match the corresponding phase of the return Doppler which is received at these same sample times.

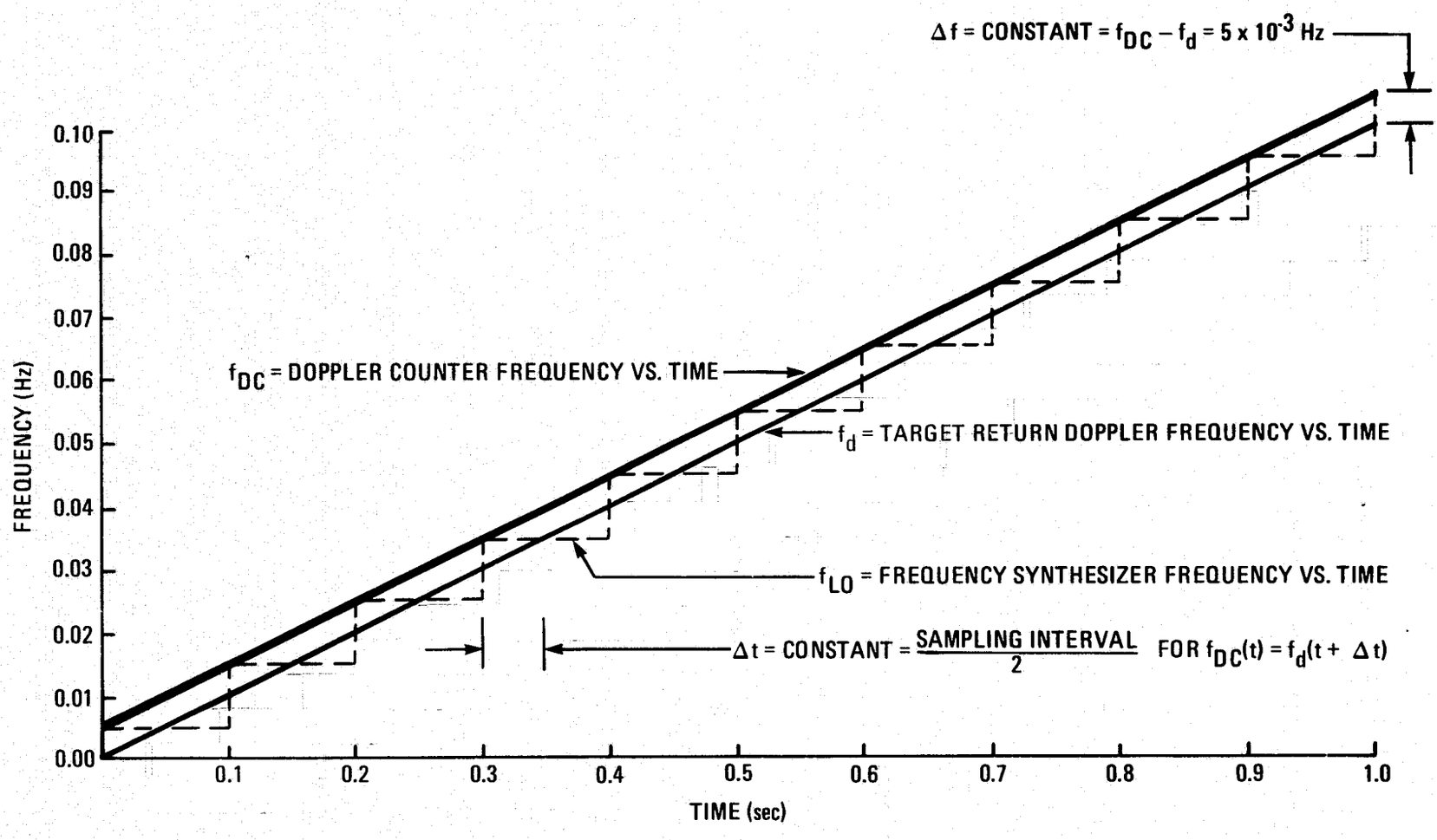

Figure 8. - Loop frequency relationships for modified model

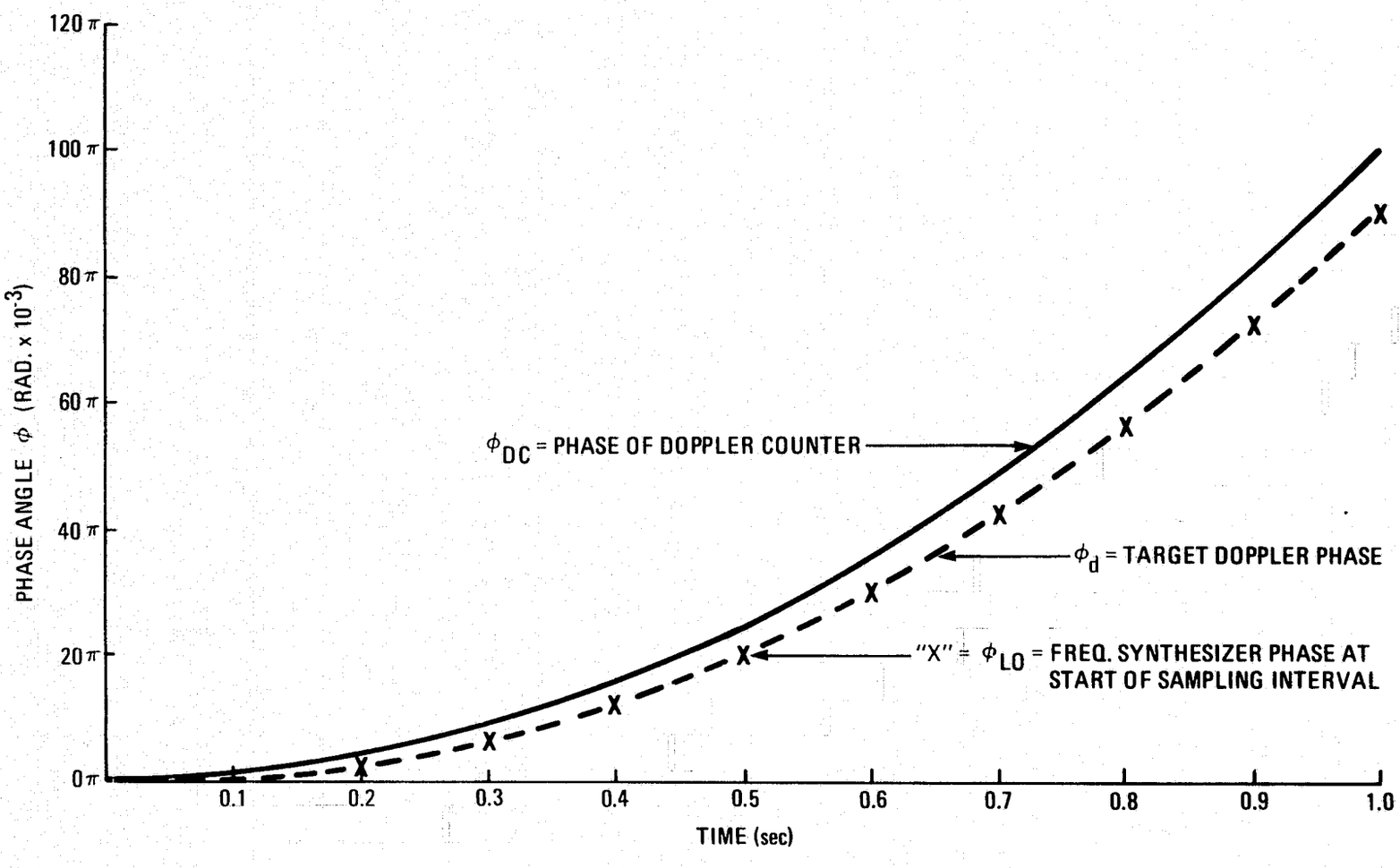

Figure 9. - Loop phase relationships for modified model

Figure 9 also shows the phase profile associated with the Doppler counter. As can be seen, the Doppler counter now exhibits a phase lead relative to the phase of true Doppler return. This Doppler counter phase lead is a linearly increasing function of time which reflects, as expected, the fact that the Doppler counter's frequency measurement (output range rate measurement) is leading (anticipating) the target's Doppler by a fixed frequency offset (0.005 Hz). While the magnitude of this offset is dependent upon the target's radial range acceleration component, the time difference between equal Doppler counter and true (target) Doppler frequencies is always fixed and equal to one-half of the synthesizer sampling interval. This result is, however, true only for a constantly accelerating target.

2.2.2 Constant Range Jerk Target

If the tracked target is assumed to have constant radial range jerk ($\dddot{R}$) component, it follows that $\ddot{R}$ will be a linear function, $\dot{R}$ a quadratic, and ϕ_d a cubic. Under these conditions, the main advantage of using a graphical approach is thus lost since the easily visualized errors associated with a linear function do not exist. Therefore, the analysis and discussion which follows will depend upon comparing tabularized results rather than comparing plotted results.

For this constant jerk target there are two main questions to be answered; what is the form of the Doppler measurement error, and, is there a form of correction similar to the $\frac{T}{2}$ time shift which will eliminate the error without requiring computation of the higher order derivatives.

Table 3 provides the computational results for an assumed constant $\dddot{R}$ target. The various columns of this table were generated as follows:

f_d = True target Doppler = $1/2\ \dddot{R}\ t^2$

$\phi_d = 2\pi \int f_d dt = \frac{2\pi}{6}\ \dddot{R}\ t^3$

T = Sampling interval = 0.1 seconds

$\Delta\phi_d$ = Change in ϕ_d between sampling intervals

TABLE II. Loop Phase and Frequency Relationships

T	t (sec)	f_d (Hz)	ϕ_d (rad x 10^{-3})	f_{DC}* (Hz)	cum ϕ_{LO}* (rad x 10^{-3})
0	0	---	---	.005	---
1	.1	0.001	π	.015	π
2	.2	0.02	4π	.025	4π
3	.3	0.03	9π	.035	9π
4	.4	0.04	16π	.045	16π
5	.5	0.05	25π	.055	25π
6	.6	0.06	36π	.065	36π
7	.7	0.07	49π	.075	49π
8	.8	0.08	64π	.085	64π
9	.9	0.09	81π	.095	81π
10	1.0	0.1	100π	.105	100π

NOTES: $f_{DC}(t=T_N) = f_{LO}(T_N \leq t < T_{N+1}) = \text{constant}$

$$\Delta\phi_{LO}(T_N \leq t < T_{N+1}) = 2\pi f_{LO}(t_N \leq t < t_{N+1})\, T$$

$$\text{cum } \phi_{LO} = \sum_{0}^{T_N} \Delta\phi_{LO}$$

ϕ_{LO} = Phase of frequency synthesizer output. For zero loop input error $\Delta\phi_{LO} = \Delta\phi_d$

$$f_{LO}(N) = \frac{1}{2\pi}\left(\frac{\Delta\phi_{LO}(N)}{T}\right) = \frac{1}{2\pi}\ \frac{\Delta\phi_d(N)}{T}$$

= The fixed frequency output from the synthesizer for N^{th} sample interval

$f_{DC}(N) = f_{LO}(N)$ = Instantaneous frequency of Doppler counter which is used to update the synthesizer at sample time (N).

$\dddot{R}$ - Constant. Arbitrarily assumed to be 0.6 Hz/sec^2

In the above listed relationships, there are two which are particularly important in the present discussion. The first is the definition of $\Delta\phi_{LO}$. Note that $\Delta\phi_{LO}$ and $\Delta\phi_d$ are defined as being equal for each sampling interval. This definition is consistent with the modified functional loop model discussed in Section 2.2.1, and precludes the possibility of a phase dependent input error being introduced into the loop. The second important relationship deals with f_{DC}. As defined, the Doppler counter frequency is forced to be at the desired LO (freq. synthesizer) frequency at the start of each sampling interval. This latter definition of f_{DC} is actually a necessary result of the $\Delta\phi_{LO} = \Delta\phi_d$ relationship and both relationships must hold for a zero-error steady state track condition.

Upon receiving the data of Table 3, it is noted that the resulting Doppler output measurement (<u>not</u> loop input) error (f_{DC}-f_d) follows a 1, 4, 7, 10, 13 ... series. The magnitude of the difference of (3×10^{-3} Hz) between these numbers per sample interval T, together with an understanding of the dynamics involved, leads to the conclusion that this linear measurement is building up according to the relationship

$$\varepsilon_1 = \left(\frac{1}{2}\ \dddot{R}\ T\right)t$$

TABLE III. Loop Relationships for $\dddot{R}$ = const. Target

T	t (sec)	f_d (Hz x 10^3)	ϕ_d/π (mr)	f_{LO} (Hz x 10^3)	f_{DC} (Hz x 10^3)	$(f_{DC}-f_d)$ (Hz x 10^3)
0	0	---	---	1	1	1
1	.1	3	0.2	7	7	4
2	.2	12	1.6	19	19	7
3	.3	27	5.4	37	37	10
4	.4	48	12.8	61	61	13
5	.5	75	25	91	91	16
6	.6	108	43.2	127	127	19
7	.7	147	68.6	169	169	22
8	.8	192	102.4	217	217	25
9	.9	243	145.8	271	271	28
10	1.0	300	200	331	331	31

The resultant error does not, however, completely account for the computed error at each sample interval. Instead, it is seen that each computed measurement error is larger by a constant factor of 1×10^{-3} Hz than would result from ε_1 alone. By assuming various sampling intervals and different assumed values of $\dddot{R}$ it is found that this constant error is a direct function of $\dddot{R}$ and varies as the square of T.

The $\dddot{R}$ and T^2 dependency and the computed magnitude lead to the conclusion:

$$\varepsilon_2 = (\tfrac{1}{6})(T)^2 \dddot{R} = \text{constant for all t}$$

The total computed measurement error is then:

$$\varepsilon(f_{DC}) = f_{DC} - f_d = \frac{T}{2} \dddot{R}\, t + \frac{T^2}{6} \dddot{R}$$

The formulation of the above measurement error completes our goal of this section. The second objective is to investigate the possibility of arriving at a general correction for the measurement error which does not depend upon knowledge of the actual target dynamics. This latter objective can best be approached by first correcting the Doppler measurement by the standard T/2 time shift, and then observing the form of the remaining residual error.

Table 4 lists the computed values of f_{DC} and f_d every T/2 seconds for the assumed target in columns 3 and 4. Column 5 of the table lists the values of f_{DC} after they have been shifted forward in time by an amount T/2 seconds (i.e. the T/2 correction has been applied). Comparing columns 4 and 5 shows that a small constant frequency error remains after the T/2 correction is applied. (This error was predicted in the mathematical analysis of section 2.1.)

TABLE IV. Effect of T/2 Correction for $\dddot{R}$ = const. Target

T	t (sec)	$f_{DC}(t)$ (Hz x 10^3)	$f_d(t)$ (Hz x 10^3)	$f_{DC}(t + T/2)$ (Hz x 10^3)
0	0	1	0	---
	0.5	3.25	.75	1
1	.1	7	3	3.25
	.15	12.25	6.75	7
2	.2	19	12	12.25
	.25	27.25	18.75	19
3	.3	37	27	27.25
	.35	48.25	36.75	37
4	.4	61	48	48.25
	.45	75.25	60.75	61
5	.5	91	75	75.25
	.55	108.25	90.75	91
6	.6	127	108	108.25
	.65	147.25	126.75	127
7	.7	169	147	147.25
	.75	192.25	168.75	169
8	.8	217	192	192.25
	.85	243.25	216.75	217
9	.9	271	243	243.25
	.95	300.25	270.75	271
10	1.0	331	300	300.25

Before proceeding, it should be noted that this present constant frequency measurement error cannot be corrected by a fixed time shift. The present Doppler frequency curve is a quadratic rather than a linear function. This quadratic form of the Doppler curve precludes the possibility of a constant frequency bias being associated with a constant time bias.

Since a time shift type of correction is precluded, it is necessary to investigate the general form of the error. By solving for the error using magnitude for $\dddot{R}$ and T it is again found that this residual error varies directly with $\dddot{R}$ and as the square of T. These results plus the magnitudes involved leads to the conclusion that:

$$\varepsilon_{f=const.} = \frac{1}{6}\left(\frac{T}{2}\right)^2 \dddot{R}$$

Thus, the T/2 time shift has over-corrected for the original time dependent error (ε_1) by a factor of 1/4. That is:

$$\varepsilon_1(t=t+T/2) = -\,1/4\varepsilon_1(t) = -\,1/8\ \dddot{R}\ T^2$$

The resulting total error is then:

$$\varepsilon_f = \varepsilon_1 + \varepsilon_2 = -\,1/8\ \dddot{R}\,T^2 + \frac{T^2}{6}\ \dddot{R} = \frac{1}{24}\,T^2\ \dddot{R}$$

While this formulation of the residual (after T/2 time shift) error does not offer a means of total error correction other than through use of $\dddot{R}$, it does allow an assessment of the error's magnitude to be made. As stated in section 2.1, a high elevation pass of the GEOS-3 satellite is associated with a maximum $\dddot{R}$ of approximately 0.3 m/sec^3. At a typical radar PRF of 160 per second (T=1/160), the peak residual Doppler measurement error after T/2 time shift) will be:

$$(1/24)\ \left(\frac{1}{160}\right)^2(0.3) = 4.9 \times 10^{-7} \text{ meters/sec}$$

It is obvious that this error is of no consequence for a target such as GEOS-3. Thus, the simple T/2 time shift correction is fully adequate for obtaining accurate Doppler data during GEOS-3 satellite tracks.

3.0 DATA CORRECTION

As described in section 2, the C-Band radar Doppler sampling error has the form:

$$\varepsilon = T/2 \dddot{R}$$

for a constantly accelerating ($\dddot{R}$=c) target.

For a constant range jerk ($\dddot{R}$=c) target the error, for all practical purposes, has the form:

$$\varepsilon = 1/2\ T \dddot{R} t$$

It is further shown in section 2 that the error for a constantly accelerating target will be completely cancelled by applying a T/2 time shift to the output Doppler data. That is,

$$f_d(\text{measured at } t=t_x-T/2) = f_d(\text{true at } t-t_x)$$

Finally, it is shown that the same T/2 time shift will also correct the measured data for the constant range jerk case. In this latter case, a small, constant measurement error will remain but its magnitude is so small that, for any practical target, it is negligible.

Therefore the easiest way to correct for the so called $\frac{PRI}{2}$ error is to time shift the output data by an amount equal to $\frac{PRI}{2}$.

Figures 10 and 11 show the results of applying a $\frac{PRI}{2}$ correction to the tracking data from GEOS-3 revolutions 212 and 498 (see Figures 1 and 2 for uncorrected residuals). In the case of revolution 498 the correction is inexact during the 640 PRF interval since a fixed 160 PRF was assumed for correction purposes. As can be seen from the corrected residuals, the T/2 time shift correction does an excellent job of illuminating this synthesizer sampling rate error.

It would, of course, also be valid to correct the data by directly applying a range rate correction which is equal in magnitude to the error. This latter approach, however, suffers from a need for either independent measurement of the higher order derivatives involved, or must rely upon first and second differences to obtain these derivatives. The a priori knowledge suffered from a reference system uncertainty error (and site translation errors) while taking 1st and 2nd differences introduce undesired noise into the solution.

It is most important to note that the PRI dependency arises from the fact that the original C-Band radar Doppler loops sample and update their local oscillator (frequency synthesizer) frequencies once each PRF. If this frequency synthesizer update rate had been at a rate 1/T seconds rather than once per PRF then the noted error would have assumed a dependency on the synthesizer update interval T rather than upon the radar's PRI.

The importance of this fact is twofold. First, both the time shift and $\dot{R}$ differences correction techniques can be most easily applied in non-real (post mission) time. This precludes the availability of accurate range rate data for real time applications. Secondly, the dependency of the error upon the interval between synthesizer update times introduces a method of easily reducing the error in real-time by merely increasing the synthesizer update rate. Thus, the error will be reduced directly for an increased synthesizer update rate for a constantly accelerating target.

In practice, it is fairly simple to obtain a greater synthesizer update rate. The original PRF update rate is derived by extracting the "-16 Kyd N^{th} Comparator Gate Trigger" train from the radar's range tracker. This pulse occurs once each PRF and is used to extract data from the Doppler counter for frequency synthesizer updating purposes. The range tracker timing circuits also have many other pulse trains available including the "64 Kyd comparator trigger" train in which 16 pulses are generated during each radar PRF. By switching from the former to the latter the Doppler counter sampling rate (synthesizer update rate) will be increased by a factor of 16:1. Even higher strobe rate signals are available but increasing the rate much further introduces the possibility of introducing synthesizer drive/switching circuit

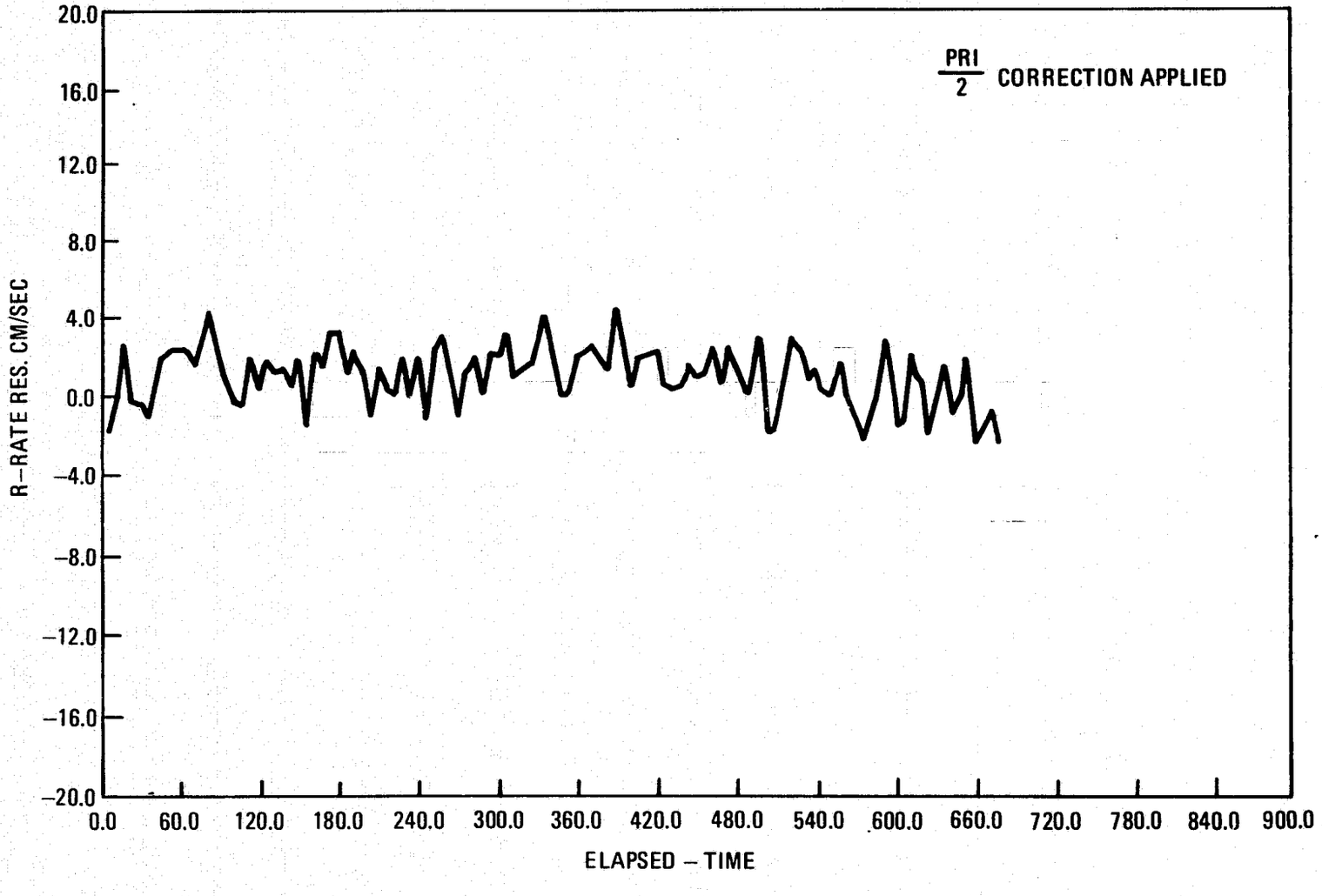

Figure 10. - Range rate residual error GEOS-3, Rev 212

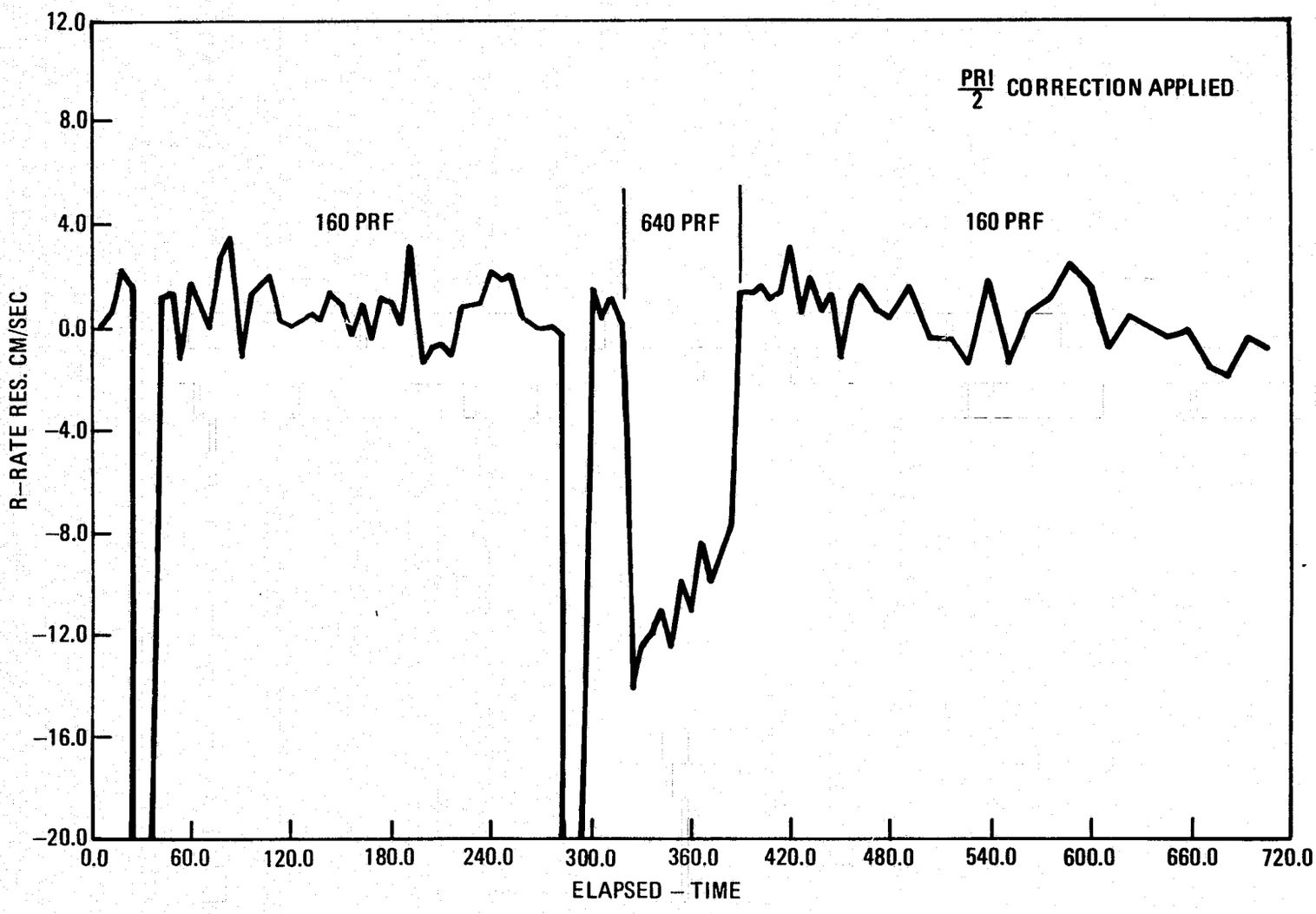

Figure 11. - Range rate residual error GEOS-3, Rev 498

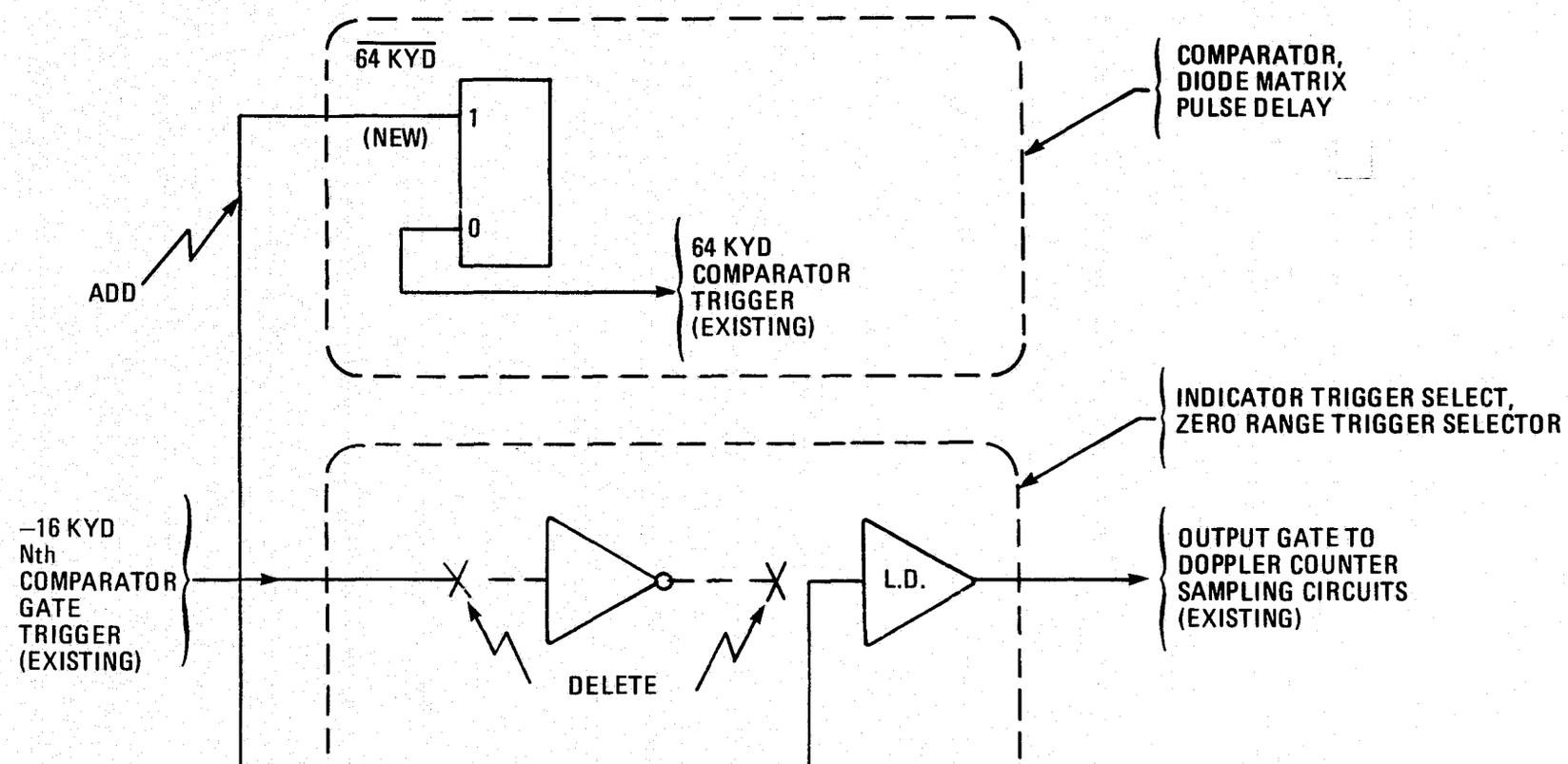

Figure 12. - CSP sampling error correction mod

heat dissipation problems. For satellite tracking purposes, a 16:1 reduction in the sampling rate error will reduce the error to the same level as the Doppler loop noise. Thus this update rate improvement seems fully adequate.

For the AN/FPQ-6 radars having the original DIRAM range trackers, the modification is quite simple as depicted in Figure 12. Similar modifications would apply to other (AN/TPQ-18, AN/FPS, AN/MPS-36) C-Band radars having Doppler tracking loops.

Figure 13 shows the Doppler tracking residuals from GEOS-3 revolution number 10510. These data were taken after implementing the modification depicted in Figure 12. The sampling rate of the frequency synthesizer has thus been increased by a factor of 16:1 which, for the PRF of 160, results in a 2560/sec synthesizer update rate. The residuals shown for revolution 10510 had no additional T/2 data correction applied. This GEOS-3 pass resulted in quite high radar elevation angles. Thus, high $\dddot{R}$ and $\ddot{R}$ components were present As can be seen, however, the resulting data have very low residual errors when compared to an earlier (Rev. 212) lower elevation pass which still used the PRF update rate. The remaining systematic error in the Rev. 10510 residuals is the result of Doppler loop dynamic lag error and not a function of the sampling rate error. (The reduced noise level in Rev. 10510 are due to post-mission filtering not used during the earlier GEOS-3 tracks.)

The lag error dependency of the Rev. 10510 systematic error is verified by the essentially flat residuals resulting from Rev. 10509 (see Figure 14) where lower target dynamics (21° max. El.) were encountered. Revolution 10509 was also tracked after the 2560/sec synthesizer update modification was implemented and, as can be seen, the resulting residual errors show no noticeable sampling rate error.

Figure 14 also shows the residuals from Rev. 212 (see Figure 1) after the $\frac{PRI}{2}$ time shift was applied. As noted before, this post-mission correction technique is also excellent. It should be noted that a post-mission T/2 correction can still be applied to the data from modified systems to effectively eliminate any remaining residual error. For systems having the 16:1 sample rate modification, this post-mission time shift becomes:

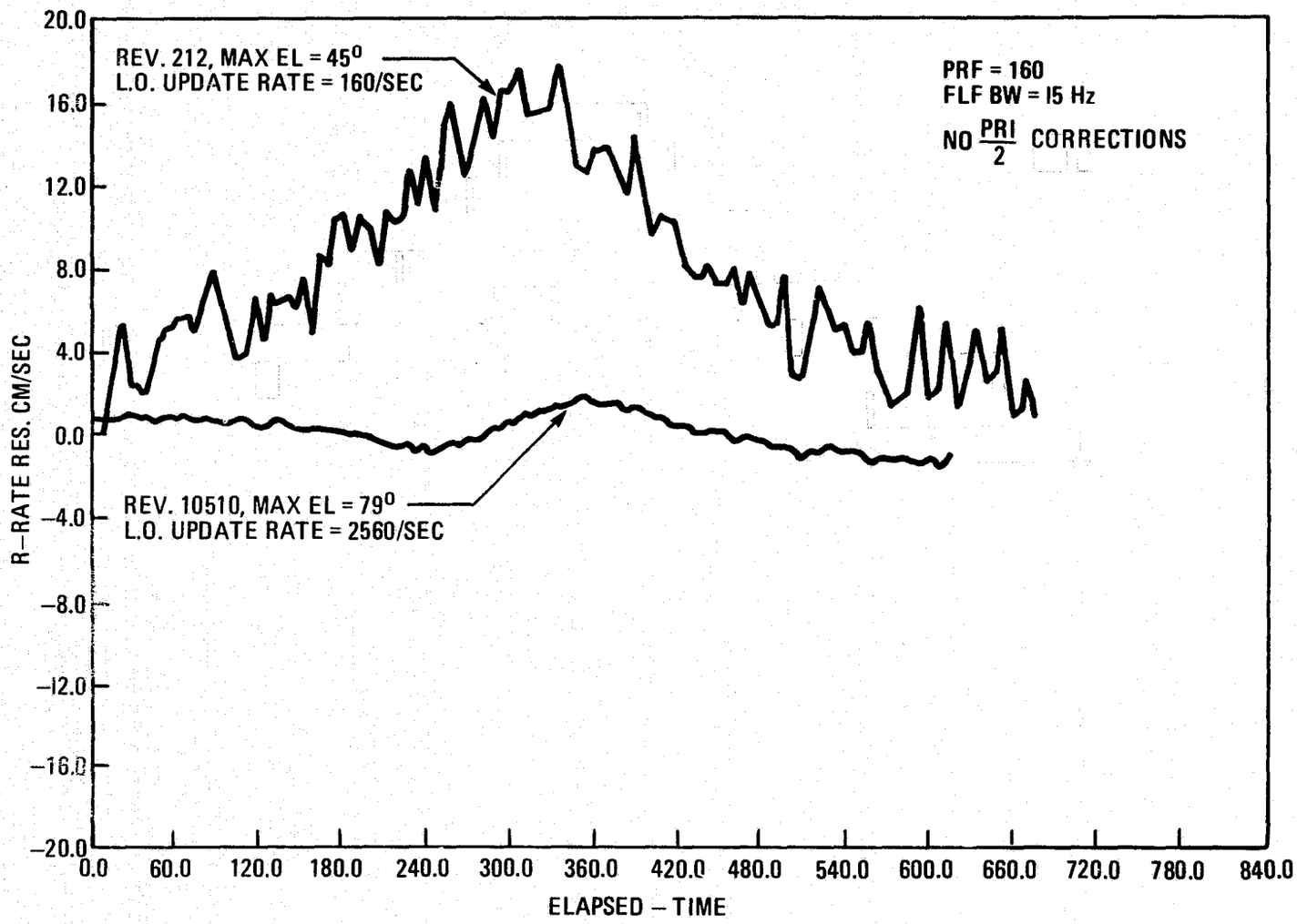

Figure 13. - Range rate residual error GEOS-3, Rev 212 and 10510

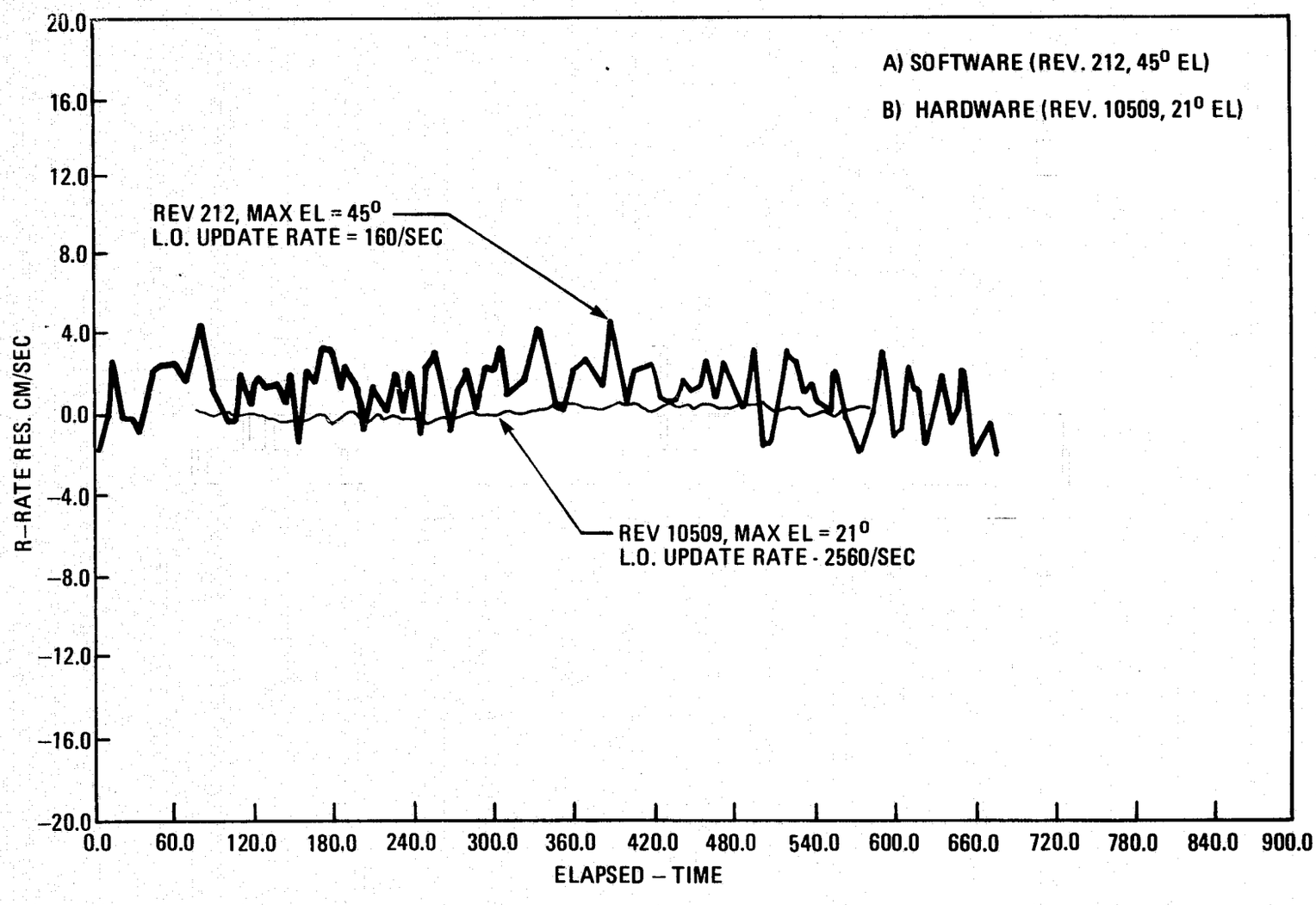

Figure 14. - Comparison of hardware and software corrections

$$f_{DC}(t-T/2) = f_{DC}(t - \frac{1}{2560 \times 2}) = f_d(t)$$

where

f_{DC} = measured (Doppler counter) target Doppler at time t.

f_d = time target Doppler at time t.

T = frequency synthesizer sampling interval.

4.0 CONCLUSION

Based upon the results of GEOS-3 satellite tracking data, it is concluded that all RCA designed C-Band radar Doppler trackers exhibit a sampling rate dependent error. In the original equipment configuration, the Doppler loop is updated once each Pulse Repetition Interval (PRI) so that the original error, for a constantly accelerating target is of the form:

$$\varepsilon(\dot{R} \text{ measured}) = \frac{PRI}{2} \ddot{R} \quad \cdot \text{ (for } \ddot{R} = C)$$

Analysis of the loop indicates that the error takes a similar form for a constant range jerk ($\dddot{R}$) target:

$$\varepsilon(\dot{R} \text{ measured}) = \frac{PRI}{2} \dddot{R}\, t + \frac{(PRI)^2}{6} \dddot{R}$$

$$\sim \frac{PRI}{2} \dddot{R}\, t$$

Analysis has shown, and tests have verified, that this sampling rate error can be corrected within a negligibly small, constant error by applying a $\frac{PRI}{2}$ time shift to the measured data. That is:

$$\text{corrected } f_d\ (t=t_x) = \text{measured } f_d\ (t=t_x - \frac{PRI}{2})$$

Having isolated the source of the error, it was further concluded that the error could be reduced in real-time by increasing the loop (frequency synthesizer) update rate. A hardware modification was subsequently implemented and tested which raised the synthesizer update rate (F) from its original rate (PRF) to a rate 16 times higher:

$$F(\text{new}) = PRF \times 16$$

The measurement error, for $\ddot{R} = C$, then becomes:

$$\varepsilon(\text{measured}) = \frac{T}{2} \ddot{R} = \frac{PRI}{32} \ddot{R}$$

Test data collected after implementation of this hardware modification verify that the sampling rate error is indeed reduced as predicted. For targets having extremely high dynamics, a further post-mission data correction can still be applied to Doppler measurements obtained from the modified loop. The necessary time shift now becomes:

$$\text{corrected } f_d \ (t=t_x) \ = \ \text{measured } f_d \ (t=tx - \frac{PRI}{32})$$

Such a correction will reduce the measurement error to a negligible amount (less than the weight of the least significant bit) for almost all conceivable targets. The residual error remaining after the corrections is:

$$(f_d \text{ corrected}) = \begin{cases} 0 \text{ for } \dddot{R} = 0 \\ \frac{1}{24} \ T^2 \ \dddot{R} \text{ for } \dddot{R} \neq 0 \end{cases}$$

where:

$$T = \frac{1}{\text{Sampling Rate}} = \begin{cases} PRI & \text{for unmodified systems} \\ \frac{PRI}{16} & \text{for modified systems} \end{cases}$$

It is recommended that all owners/users of C-Band pulse Doppler systems apply the time shift correction:

$$\text{shifted time tag} \ = \ \text{measurement time tag} + \frac{T}{2}$$

as a minimum. Further, it is recommended that steps be taken to modify the applicable radars to incorporate the 16:1 increase in loop update rate as discussed in section 3.

Finally, for users desiring the best possible data, it is recommended that the time shift correction still be applied to the Doppler measurements extracted from modified systems. The time shift value must, however, reflect the increased update rate and thus becomes:

$$\Delta t = (1/16) \left(\frac{PRI}{2}\right)$$

and, for modified systems:

Shifted time tag = measurement time tag + Δt

REFERENCES

1. Flight Test Data Analysis Program Radar Performance Parameter Data Final Report, July 1970, Contract No. F04701-69-C-0131.

2. Kuo, Benjamin C., Analysis and Synthesis of Sampled Data Control Systems, Prentice-Hall, Inc., Englewood Cliffs, N. J. 1963.

3. Tou, Julius T., Digital And Sampled-Data Control Systems, McGraw-Hill Book Co., Inc., New York, 1959.

1. Report No.	2. Government Accession No.	3. Recipient's Catalog No.
NASA TM-69366		

4. Title and Subtitle	5. Report Date
C-BAND RADAR PULSE DOPPLER ERROR ITS DISCOVERY, MODELING, AND ELIMINATION	February 1978
	6. Performing Organization Code

7. Author(s)	8. Performing Organization Report No.
W. B. Krabill (NASA Wallops Flight Center) D. J. Dempsey (RCA Missile and Surface Radar Division)	
	10. Work Unit No.

9. Performing Organization Name and Address	11. Contract or Grant No.
NASA Wallops Flight Center, Wallops Island, VA 23337 and RCA Missile and Surface Radar Division, Moorestown, NJ 08057	NAS6-2637
	13. Type of Report and Period Covered
12. Sponsoring Agency Name and Address	Technical Memorandum
National Aeronautics and Space Administration Wallops Flight Center Wallops Island, VA 23337	14. Sponsoring Agency Code

15. Supplementary Notes

16. Abstract

The discovery of a C-Band radar pulse Doppler error is discussed and use of the GEOS-3 satellite's coherent transponder to isolate the error source is described.

An analysis of the pulse Doppler tracking loop is presented and a mathematical model for the error is developed.

Error correction techniques are developed and described including implementation details.

17. Key Words (Suggested by Author(s))	18. Distribution Statement
Tracking GEOS-3	Unclassified - unlimited. STAR Category 32

19. Security Classif. (of this report)	20. Security Classif. (of this page)	21. No. of Pages	22. Price*
Unclassified	Unclassified	49	

*For sale by the National Technical Information Service, Springfield, Virginia 22151